AGU PUBLICATIONS

Geophysical Research Letters

RESEARCH LETTER
10.1002/2016GL069840

Special Section:
First results from NASA's Magnetospheric Multiscale (MMS) Mission

Inverse energy dispersion of energetic ions observed in the magnetosheath

S. H. Lee[1], D. G. Sibeck[1], K.-J. Hwang[1,2], Y. Wang[3], M. V. D. Silveira[1], M.-C. Fok[1], B. H. Mauk[4], I. J. Cohen[4], J. M. Ruohoniemi[5], N. Kitamura[6], J. L. Burch[7], B. L. Giles[1], R. B. Torbert[8], C. T. Russell[9], and M. Lester[10]

[1]NASA Goddard Space Flight Center, Greenbelt, Maryland, USA, [2]Goddard Planetary and Heliophysics Institute, University of Maryland, Baltimore County, Baltimore, Maryland, USA, [3]Institute of Space Physics and Applied Technology, School of Earth and Space Sciences, Peking University, Beijing, China, [4]The Johns Hopkins University Applied Physics Laboratory, Laurel, Maryland, USA, [5]Bradley Department of Electrical and Computer Engineering, Virginia Polytechnic Institute and State University, Blacksburg, Virginia, USA, [6]Institute of Space and Astronautical Science, Japan Aerospace Exploration Agency, Sagamihara, Japan, [7]Southwest Research Institute, San Antonio, Texas, USA, [8]Space Science Center, University of New Hampshire, Durham, New Hampshire, USA, [9]Department of Earth and Space Sciences, University of California, Los Angeles, California, USA, [10]Department of Physics and Astronomy, University of Leicester, Leicester, UK

Key Points:
- A burst of energetic proton, helium, and oxygen ions that exhibited an inverse dispersion was observed by MMS in the magnetosheath
- The observed inverse energy dispersion signatures can be caused by betatron acceleration that energizes the energetic magnetospheric ions
- The energetic ions can escape through reconnection that can be triggered by a transient solar wind dynamic pressure pulse

Correspondence to:
S. H. Lee,
sun.h.lee@nasa.gov

Citation:
Lee, S. H., et al. (2016), Inverse energy dispersion of energetic ions observed in the magnetosheath, *Geophys. Res. Lett.*, *43*, 7338–7347, doi:10.1002/2016GL069840.

Received 31 MAY 2016
Accepted 2 JUL 2016
Accepted article online 8 JUL 2016
Published online 22 JUL 2016

Abstract

We present a case study of energetic ions observed by the Energetic Particle Detector (EPD) on the Magnetospheric Multiscale spacecraft in the magnetosheath just outside the subsolar magnetopause that occurred at 1000 UT on 8 December 2015. As the magnetopause receded inward, the EPD observed a burst of energetic (~50–1000 keV) proton, helium, and oxygen ions that exhibited an inverse dispersion, with the lowest energy ions appearing first. The prolonged interval of fast antisunward flow observed in the magnetosheath and transient increases in the *H* components of global ground magnetograms demonstrate that the burst appeared at a time when the magnetosphere was rapidly compressed. We attribute the inverse energy dispersion to the leakage along reconnected magnetic field lines of betatron-accelerated energetic ions in the magnetosheath, and a burst of reconnection has an extent of about 1.5 R_E using combined Super Dual Auroral Radar Network radar and EPD observations.

1. Introduction

Bursts of energetic (>50 keV) particles are common in the magnetosheath. Both the solar wind and the Earth's magnetosphere can contribute to this population [*Crooker et al.*, 1981; *Sibeck et al.*, 1987b; *Fuselier et al.*, 1991; *Kudela et al.*, 1992]. The two possible sources have different acceleration and transport mechanisms. The drift paths of energetic ions and electrons in the outer magnetosphere encounter the magnetopause, where these particles can be lost to the magnetosheath by scattering [*Roederer*, 1970] and leakage or escape along reconnected magnetic field lines [*Scholer et al.*, 1981; *Sibeck et al.*, 1987b, 1988]. By contrast, solar wind ions can be accelerated at the quasi-parallel bow shock (Fermi acceleration) and swept into the magnetosheath [*Lee*, 1982; *Fuselier et al.*, 1991; *Freeman and Parks*, 2000].

Ion energy-dispersed signatures have often been observed within the Earth's magnetosphere [*Quinn and McIlwain*, 1979; *Quinn and Southwood*, 1982; *Mauk*, 1986; *Sauvaud et al.*, 1999]. Several possible causes of the dispersions have been suggested. The first possible cause of the energy dispersion is a time-of-flight (TOF) effect (temporal effect). Higher energy ions drift faster and reach an observing spacecraft before lower energy ions. If the more energetic ions reach the magnetopause first and leak out, a spacecraft in the magnetosheath might observe a direct dispersion with more energetic ions arriving first. Energy-dispersed ion signatures are frequently observed in the dayside magnetosphere following geomagnetic substorms [*Reeves et al.*, 1990]. Finite Larmor radius effects (spatial effects) can also cause normal energy-dispersed ions near the magnetopause. The higher energy ions reach locations farther outside the magnetopause thanks to their larger Larmor radii. A spacecraft moving from the magnetosheath to the magnetosphere might therefore observe more energetic particles first, resulting in a direct dispersion effect.

In this paper, we report a clear inverse energy dispersion (lowest energies observed first) signature observed in the magnetosheath near the subsolar magnetopause by the EPD on the Magnetospheric Multiscale (MMS)

spacecraft on 8 December 2015. We describe how the inverse energy dispersions of energetic ions (>50 keV) occur and describe a possible new mechanism. We use simultaneous MMS observations and ground magnetometer data to investigate the mechanism responsible for producing the observed inverse energy dispersion signature and to obtain evidence for reconnection triggered by a transient solar wind dynamic pressure pulse. We also estimate the longitudinal extent of the reconnection line on the basis of the MMS observations of a burst of energetic ions, ground magnetometer observations, and Super Dual Auroral Radar Network (SuperDARN) radar data.

A possible scenario is that a transient localized solar wind dynamic pressure impulse drives a burst of reconnection and poleward convection of a group of newly reconnected magnetic field lines in the ionosphere. The inverse energy dispersion signatures can be caused by betatron acceleration that energizes the energetic magnetospheric ions just before they escape from the magnetosphere.

2. MMS Observations

This paper presents simultaneous MMS, Acceleration, Reconnection, Turbulence and Electrodynamics of Moon's Interaction with the Sun (ARTEMIS), SuperDARN radar, and ground magnetometer observations. The four MMS spacecraft were located just duskward from the subsolar magnetopause near $(X, Y, Z)_{GSM}$ = (11.1, 0.6, −1.2) R_E at the time of the event from 0900 UT to 1100 UT on 8 December 2015.

Figure 1 presents an overview of the event. Figures 1a–1c show interplanetary parameters measured by ARTEMIS P2, which were shifted by 3 min 30 s to account for propagation time from the ARTEMIS P2 to the MMS position. We calculated the time shift by matching the magnetosheath clock angles observed by MMS (black) and the upstream interplanetary magnetic field (IMF) clock angles measured by ARTEMIS P2 (red), which are well matched at 1025 UT, 1035 UT, and 1042 UT (black arrows) shown in Figure 1d. Figures 1e–1p show an overview of magnetic field and plasma data from MMS 2. ARTEMIS P2 was upstream of the dawn bow shock at $(X, Y, Z)_{GSM}$ = (49.4, −35.7, 13.8) R_E. The x component of the interplanetary magnetic field (IMF) was dominant (radial IMF), and there was a southward IMF (IMF $B_z < 0$) (Figure 1a). The geomagnetic activity indices (*Dst* and *Kp*) were about −24 nT and 2, respectively, indicating that geomagnetic conditions were quiet (not shown). ARTEMIS observations provide no evidence for any sudden pressure (or density) change during the time period of interest (shaded region) from 0952:30 UT to 0959:30 UT (Figures 1b and 1c). The MMS spacecraft were on the inbound leg of their orbit near local noon. The color bars above Figure 1e indicate the magnetosphere (Msp) and magnetosheath (Msh) regions, which can be distinguished by the field strength and orientation, energy spectra, and density profiles. Figures 1e–1j show *GSM* components of the magnetic field measured by the fluxgate magnetometers (FGM) [*Torbert et al.*, 2014; *Russell et al.*, 2014], the energy-time spectrogram for ions, the energy-time spectrogram of electrons, the ion density, the ion bulk velocity components, and the total pressure, as observed by the fast plasma investigation (FPI) instrument [*Burch et al.*, 2015]. Figures 1k–1p present the energy-time spectrograms and pitch angle distributions of the energetic ions (hydrogen, helium, and oxygen ions) measured by the energetic ion spectrometer (EIS) sensor [*Mauk et al.*, 2014]. The EIS sensor measures electrons and ions by energy, direction, and species with a time resolution of ~2.5 s in survey mode used here. Pitch angle distributions are obtained once per spin (~20 s). The shaded region represents a very unusual magnetopause crossing where all three ion species exhibited inversely energy-dispersed ions in the magnetosheath (Figures 1k, 1m, and 1o). An inverse dispersion occurs when lower energy ions appear earlier than higher energy ions. A strong antisunward V_x flow (~400 km/s) accompanied the inverse energy dispersions (Figure 1i). The energetic ions in the inverse dispersions (shaded region) had >90° pitch angles (Figures 1l, 1n, and 1p). The sudden increase in V_x flow indicates rapid earthward motion of the magnetopause. A high-speed flow in the southward direction, $V_z = -150$ km/s, was observed from 0956 UT to 0957 UT (Figure 1i). It satisfies the Walén relation since the flow velocity in de Hoffmann-Teller frame is highly correlated (0.75) with the local Alfvén velocity from 0955:20 UT to 0957:00 UT (not shown). This indicates that the spacecraft was south of a reconnection line when the magnetopause was encountered.

We want to determine the source of the ions in the inverse dispersion. Figure 2 shows three-dimensional polar versus azimuthal angle distributions of proton (left column), helium (middle column), and oxygen (right column) ions in the 1000:40 UT–1001:00 UT (top row) and 1002:17 UT–1002:37 UT (bottom row) time intervals (~20 s spin period). The white solid lines indicate contours of constant pitch angles as determined from the instantaneously measured magnetic field. The ion flux levels are color coded with brighter colors representing higher fluxes. These angular distributions show that the maximum ion fluxes come from the south (negative

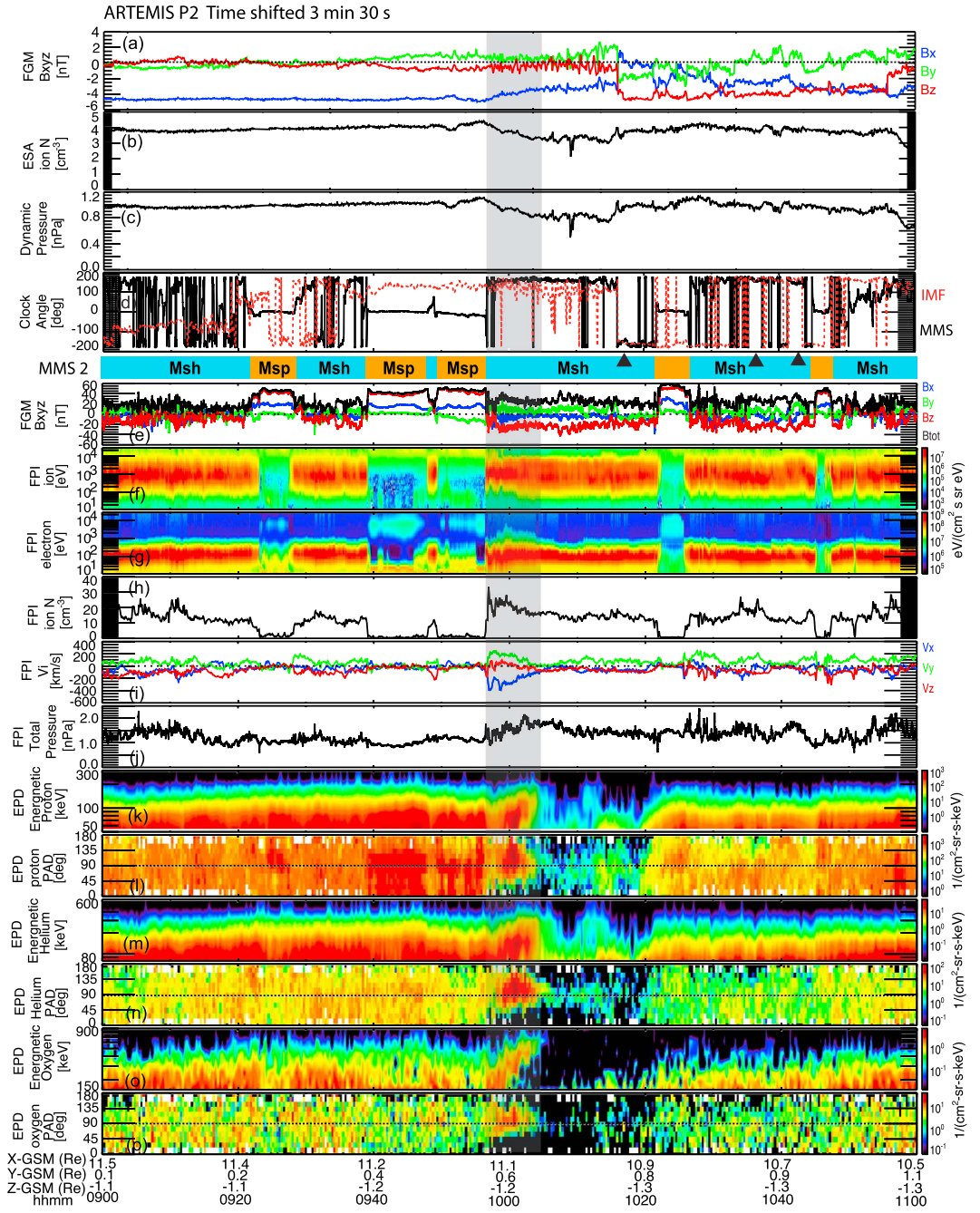

Figure 1. (a) The IMF, (b) the ion number density, and (c) the solar wind dynamic pressure measured by ARTEMIS P2, shifted by 3 min 30 s for the propagation time from ARTEMIS P2 to MMS. (d) The clock angles measured by MMS (black) are compared to the IMF clock angles observed by ARTEMIS P2 (red). (e) The magnetic field components in *GSM* coordinates, (f) the ion energy flux spectrum, (g) the electron energy flux spectrum, (h) the ion density, (i) the ion velocity components, (j) the total pressure, (k) energetic (50–300 keV) proton energy spectrum, (l) energetic proton pitch angle distribution, (m) energetic (80–600 keV) helium energy spectrum, (n) energetic helium pitch angle distribution, (o) energetic (150–900 keV) oxygen energy spectrum, and (p) energetic oxygen ion pitch angle distribution. Note that the charge states of the helium and oxygen ions are not measured. The magnetopause crossing associated with the observation of unusual inversely energy-dispersed energetic ions in the magnetosheath is denoted by the shaded area.

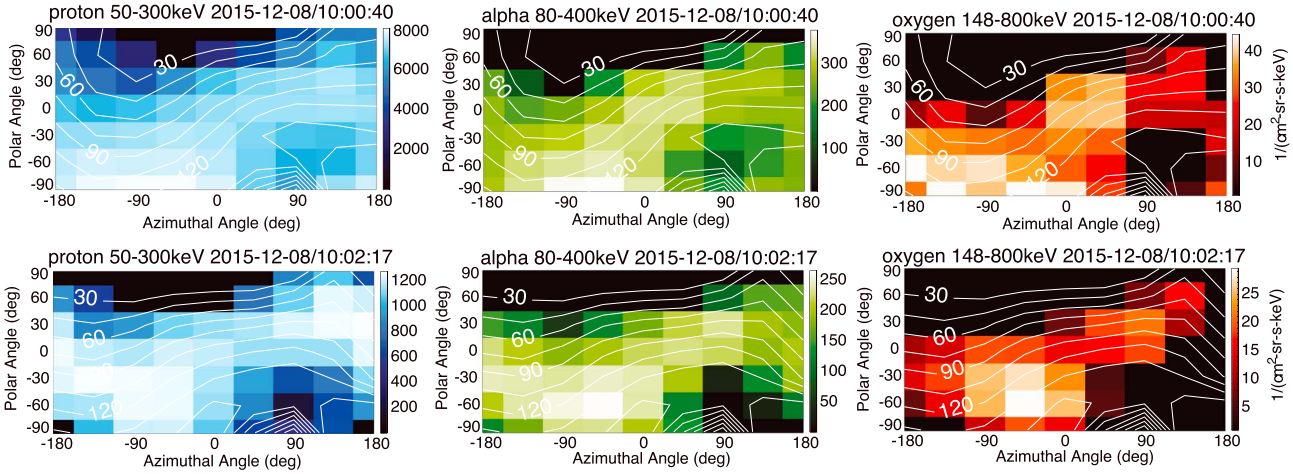

Figure 2. (left column) Energetic proton, (middle column) helium, and (right column) oxygen ion angular distributions (polar versus azimuthal angle). The white lines show contours of constant pitch angles.

polar angle) and dawnside (negative azimuth angle). Since ions with gyrocenters closer to the magnetosphere would arrive from these directions for the observed duskward and antisunward magnetosheath magnetic fields, the origin of the observed energetic ions in the magnetosheath is the magnetosphere. We therefore exclude any significant contribution of the solar wind to the energetic ion populations observed in the magnetosheath.

3. Interpretation and Discussion

3.1. How Do Inverse Dispersions of Energetic Ions in the Magnetosheath Occur?

We considered two possible mechanisms for producing the burst of inversely dispersed energetic ions observed in the magnetosheath near the magnetopause: (1) a substorm injection with spatial effects and (2) a transient solar wind dynamic pressure pulse.

Substorms inject particles into the inner magnetosphere and energize particles through betatron and/or Fermi acceleration processes [*Sauvaud et al.*, 1999; *Kazama and Mukai*, 2003]. The injected energetic particles drift from the nightside to the dayside magnetosphere. If the burst of the energetic ions observed just outside the magnetopause near local noon results from a substorm injection, then we expect to find a substorm injection signature in the magnetotail at a reasonable drift time before the magnetopause event.

At the time of this event, Time History of Events and Macroscale Interactions During Substorms (THEMIS) A was located near local midnight in the magnetotail near $(X, Y, Z)_{GSM} = (-11.7, -1.5, -2.7)$ (not shown). There was a clear increase in the ground-based THEMIS pseudo-*AE* index (~250 nT) and in the THEMIS A x component of ion bulk velocity (~350 km/s) from 0850 UT to 0910 UT, indicating a substorm onset and earthward plasma (ion and electron) motion. The flux of energetic particles (<100 keV) at THEMIS A increased, also indicating a substorm injection. The drift time from the nightside to the dayside for 70 keV (90 keV) protons with 90° pitch angles is about 44 min (34 min) at $L = 8$ using a simple dipole field model, somewhat less than that required to explain any connection to MMS (1 h). Because the real drift time may be somewhat different than our estimate, it is entirely possible that these injected magnetospheric ions can be the source population for the inverse dispersion of energetic ions observed in the magnetosheath.

Mechanism 1 combines a substorm injection and spatial effects. The injected magnetospheric ions escape into the magnetosheath via reconnected field lines (model 1a) and/or via a leakage process (model 1b). In model 1a, the lower energy ions would have to be observed close to the magnetopause, while the higher energy ions are detected farther from the magnetopause on the recently reconnected field lines [e.g., *Zong et al.*, 2001]. In model 1b, magnetospheric ions drift to the magnetopause and leak out into the magnetosheath by finite gyroradius effects [*Sibeck et al.*, 1987b; *Sibeck and McEntire*, 1988; *Zong and Wilken*, 1998; *Zong et al.*, 1999]. The more energetic (faster) ions have larger gyroradius and reach locations farther from the magnetopause than the less energetic ions at any given time.

As described by *Zong et al.* [2001], model 1a can predict inverse and forward dispersions depending on the motion of the spacecraft relative to layers of particles at the magnetopause. We expect ions with different species and different energies to be simultaneously observed if multiple species reach the observing spacecraft with the same velocity [*Zong et al.*, 1999]. The energies of helium and oxygen ions should be 4 and 16 times higher than the energy of proton to be observed simultaneously. However, the characteristic energies of proton, helium, and oxygen ions which have high fluxes at 1002 UT are 120 keV, 200 keV, and 400 keV, respectively, from our observations. The corresponding velocities of proton, helium, and oxygen ions with these characteristic energies are about 4800 km/s, 4380 km/s, and 2190 km/s, respectively, which indicates that they cannot reach the observing spacecraft at the same time. Therefore, model 1a, injection and spatial effect, cannot explain our inverse energy dispersions.

As described by *Zong and Wilken* [1998] and *Zong et al.* [1999], model 1b predicts that the oxygen ions extend farther from the magnetopause than layers of proton and helium ions, since oxygen ions have gyroradii about four and two times larger than proton and helium ions, respectively, at the same energy. We observe proton, helium, and oxygen ions with characteristic energies of 120 keV, 200 keV, and 400 keV, respectively, corresponding to gyroradii of about 0.16 R_E, 0.29 R_E, and 1.15 R_E, respectively. To see all three species with these energies at once, the spacecraft must be within 0.16 R_E of the magnetopause. The spacecraft should be able to observe oxygen ions with energies less than 400 keV and helium with energies less than 200 keV at the moment. Yet they are not observed. Therefore, model 1b cannot explain our inverse dispersion events either.

Now consider the observed rapid inward magnetopause motion and the possibility that a transient solar wind dynamic pressure pulse (model 2) might have been the cause of the inverse energetic particle dispersion. The energetic ions injected by the magnetotail substorm are energized via betatron acceleration, while the solar wind dynamic pressure pulse compresses the magnetosphere. As the magnetosphere is progressively compressed, the energy of the escaping ions increases so that an inverse dispersion is observed in the magnetosheath just outside the magnetopause. *Wilken et al.* [1982, 1986] showed that the sudden compression of the magnetosphere induced by an interplanetary shock arriving at the subsolar magnetopause had an effect on the energies of the magnetospheric energetic particles. They proposed that the hydromagnetic waves (step-like waves), which were generated during the compression, propagated into the magnetosphere and energized the local energetic particle distributions.

We might have expected to see a dramatic sudden increase in the solar wind dynamic pressure corresponding to this motion. However, the ARTEMIS observations in Figure 1c show no such increase within 1 h. Note, however, that the IMF was nearly radial during the time period of interest from 0900 to 1100 UT. Past work indicates that strong (factor of 2–3 or more) pressure pulses can be generated within the foreshock during intervals of radial IMF [*Fairfield et al.*, 1990]. The pressure pulses can cause large-amplitude magnetopause motion when they strike the magnetosphere [*Sibeck et al.*, 1989]. Consistent with this expectation, Figure 1j shows that the total pressure within the magnetosheath increased by a factor of ~2 from 0958 UT to 1002 UT.

The estimated magnetopause location (R) after a compression can be written as $R_f \approx (R_i - V_n * T)$, where V_n and T represent the velocity of the magnetopause and the duration of the compression, which is about 4 min from 0958 UT to 1002 UT. We used multipoint timing to determine an inward magnetopause velocity (V_n) of 75 km/s. The subscripts "i" and "f" denote, respectively, the quantities before and after the compression. Assuming a constant inward velocity, we obtain an inward magnetopause displacement of $V_n * T \approx\sim 2.8\, R_E$. Since dipolar magnetospheric magnetic field strengths within the subsolar magnetopause vary as the inverse cube of the distance to the magnetopause, the increase in the subsolar magnetospheric magnetic field strength corresponding to the compression is on the order of as $B_f/B_i \approx (R_i/R_f)^3 \approx\sim 2.4$. Conservation of the first adiabatic invariant then requires energetic ion energies just inside the magnetopause to increase by a factor of 2.4 during the compression (betatron acceleration). As can be seen in Figures 1k, 1m, and 1o, the energies at which the fluxes of energetic ions escaping from the magnetosphere peak indeed increased by a factor of ~2. The energy at which the proton flux peaks increased approximately from 60 keV to 120 keV, helium from 100 keV to 200 keV, and oxygen from 200 keV to 400 keV.

They maintain their energy upon streaming into the magnetosheath. Although the magnetosheath is a region of weaker magnetic field strength, these ions conserve the first adiabatic invariant while escaping. Consequently, the pitch angles decrease from 90° to ~130° (or ~50°) as they move along the magnetic field from 50 nT magnetospheric field strengths to 30 nT magnetosheath magnetic field strengths, assuming that the

energetic magnetospheric ions were drifting with 90° pitch angles in the magnetosphere (Figures 1l, 1n, and 1p).

We can also find evidence for the effect of the solar wind dynamic pressure impulse on the magnetosphere in low-latitude ground magnetograms. The geomagnetic responses to solar wind pressure changes are readily detected by equatorial stations [e.g., *Sibeck*, 1993]. We used ground magnetometer data from the low-latitude magnetic stations of International Real-Time Magnetic Observatory Network (INTERMAGNET) and African Meridian B-Field Education and Research (AMBER) network: Guitar-Tenerife (GUI), Tamanrasset (TAM), Mbour (MBO), Conakry (CNKY), and Abidjan (ABAN). We found that the horizontal (H) component geomagnetic field, pointing northward, suddenly increases at the same time as the energetic ions were observed in the magnetosheath (not shown). The magnetic pulse observations in the ground magnetograms coincide with the inversely energy-dispersed ions seen by the MMS spacecraft, confirming that a transient pressure pulse caused the inward magnetopause motion and energization of the injected magnetospheric ions.

3.2. Particle Escape and the Extent of the Reconnection Line

There are several ways by which energetic magnetospheric particles can escape into the magnetosheath. Reconnection is one escape mechanism that allows energetic particles to stream into the magnetosheath along interconnected magnetosheath and magnetospheric magnetic field lines. We can use MMS observations, ground magnetometer data, and ionospheric data from the SuperDARN radar network to determine the characteristics of reconnection and in particular the length of the reconnection line for this event. The International Monitor for Auroral Geomagnetic Effects (IMAGE) magnetometers, the SuperDARN radars at Hankasalmi (HAN) in Finland, and MMS are all located near local noon around 1000 UT.

In addition to the reconnection-related flows (V_z) seen by MMS in situ at the magnetopause, ground-based radars and magnetometers provide evidence for reconnection on this event. Figure 3 presents observations by IMAGE, SuperDARN, and the MMS spacecraft. Figure 3 (first panel) shows the Y component (east-west component) of the magnetic field at the high-latitude magnetic stations in the IMAGE magnetometer network (NAL, LYR, HOR, BJN, and NOR) from 0900 UT to 1100 UT. The magnetic stations are ordered downward by decreasing latitude. There are positive Y component perturbations in each high-latitude magnetogram. The peaks appear to propagate poleward. The eastward ($Y > 0$) magnetic field perturbations are caused by southward currents and therefore poleward convection flows (antisunward flows) that are associated with a burst of reconnection at the dayside magnetopause.

The Northern Hemisphere SuperDARN radars at HAN in Finland can also be used to study the response of the ionospheric convection at high latitudes to a burst of reconnection at the dayside magnetopause. Figure 3 (second to fourth panels) shows the line-of-sight velocities from the HAN radar with color coding according to the scales measured in three beam directions (Beams 10, 8, and 6). The lowest beam number is directed toward the west. The gray region represents the ground scatter, reflection from the ground. The colored regions depict the ionospheric scatter. The red and orange colors depict velocities moving away from the radar, while blue and green colors correspond to velocities moving toward the radar. A strong negative (poleward) flow was observed between 75° and 80° magnetic latitudes and moved westward as indicated by the arrow. This poleward velocity is consistent with the positive Y deflection observed by the ground magnetometers. Previous studies have found that poleward ionospheric flows are associated with localized bursts of reconnection at the dayside magnetopause [*Pinnock et al.*, 1993; *Lockwood et al.*, 1993]. The westward motion of the flow region is associated with the poleward motion of the magnetic field perturbations.

Zong et al. [2001] suggested that oxygen ions from the ring current can escape into the magnetosheath along reconnected field lines. They argued that the region of reconnection line through which energetic ions escape depends upon their longitudinal drift velocities. *Zong et al.* [2001] reported observations of only energetic oxygen ions (~250 keV) in the magnetosheath during storm time. No hydrogen or helium ions were detected. They concluded that the observations were made at a location along the reconnection line that only oxygen and not hydrogen or helium ions could reach. Since oxygen ions drift farther westward in one bounce than either protons or helium ions, cases in which only escaping oxygen ions can be observed are expected. Since energetic ions will be lost within one bounce, they cannot be observed at distances greater than their gradient curvature drift in one bounce period from the duskward edge of reconnection line.

We can determine the finite longitudinal extent of the reconnection line at 1000 UT using the MMS observations and ionospheric data from the SuperDARN radar network if the ion drift model suggested by *Zong et al.*

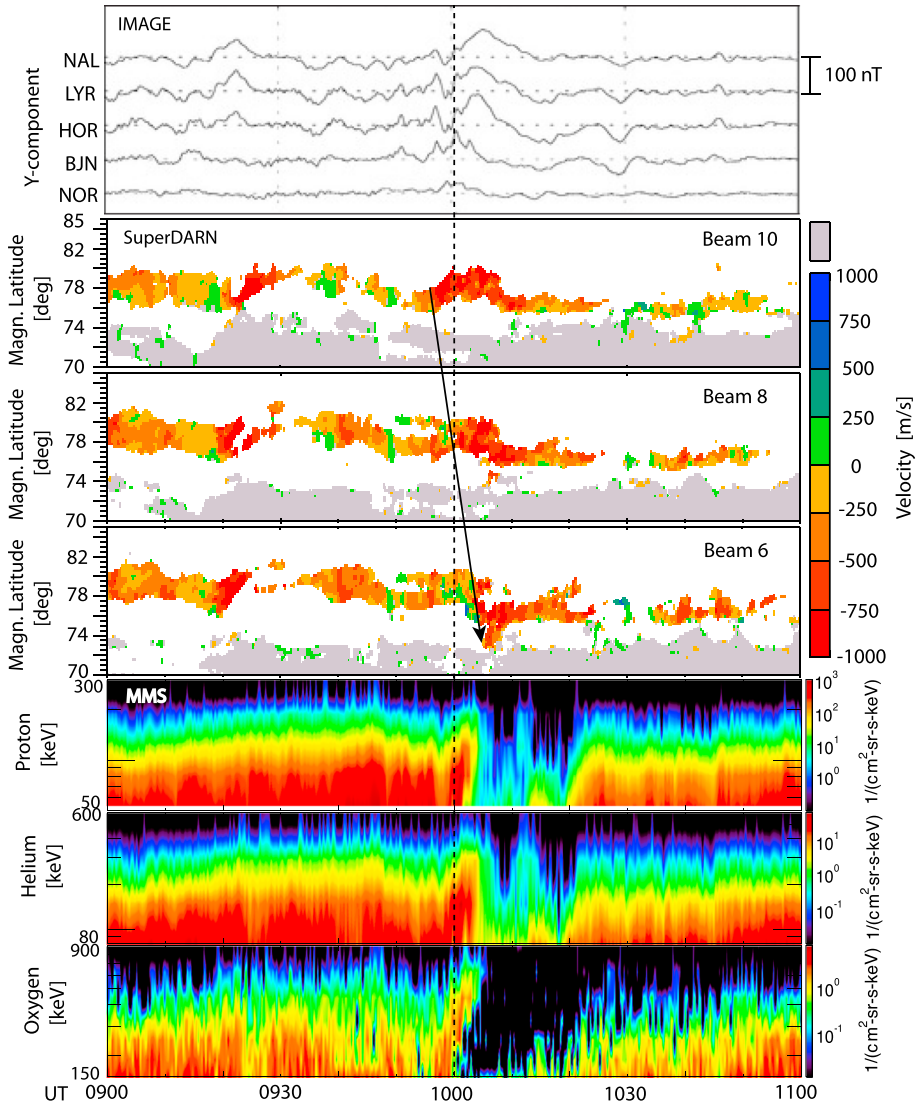

Figure 3. (first panel) The *Y* component of the ground magnetic field as measured by ground magnetometers located at NAL, LYR, HOR, BJN, and NOR (IMAGE chain). (second to fourth panels) The line-of-sight Doppler velocity measured by the Hankasalmi (HAN) radar (beams 10, 8, and 6, respectively). (fifth to seventh panels) The energetic ion energy spectrograms measured by EPD-EIS.

[2001] is correct. The combined electric field and gradient curvature drift paths of energetic ions depend on their energies, charges, and pitch angles. Ions with higher energies (>25 keV) predominantly follow the gradient curvature drift paths. Ions with near 90° pitch angles drift outward on the dayside and are more likely to encounter the magnetopause than ions with lower pitch angles [*Sibeck et al.*, 1987a]. Energetic ions with different energies and pitch angles reach different magnetopause locations. We assumed that the drift paths of energetic proton, helium, and oxygen ions at their different, but large, characteristic energies are identical. MMS observed an inversely energy-dispersed ion pattern in all three ion populations. The expected longitudinal drifts during the bounce period of a singly charged 400 keV oxygen ion, a doubly charged 200 keV helium ion, and a singly charged 120 keV proton in a dipole field at $L = 8$ are about 3.7 R_E, 0.9 R_E, and 0.5 R_E, respectively. Since MMS observed all three simultaneously in the magnetosheath, the distance of the observing spacecraft from the eastern edge of the reconnection line should not be more than 0.5 R_E (Figure 4a). Figure 4a shows a schematic of particle drift, bounce motions, and particle escape through the reconnection line. Since MMS was at $(X, Y, Z) = (11.1, 0.6, -1.2)$ R_E, the eastern edge of the reconnection line could not have been any farther eastward than $(11.1, 1.1, -1.2)$ R_E.

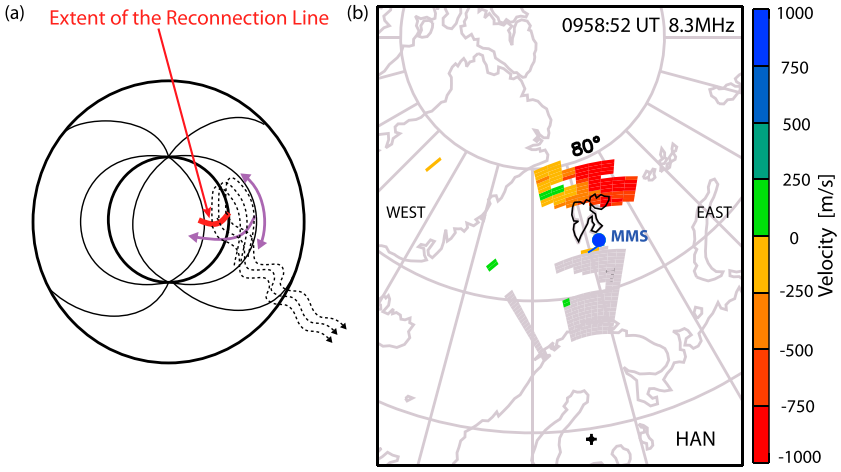

Figure 4. (a) A schematic view of the magnetosphere illustrating how the trajectories of energetic ions (dashed lines) intersect the reconnection line (red line) and escape within one bounce period. (b) Radial velocity map from the HAN radar 0958:52 UT with footprints of the MMS spacecraft from 0957 UT to 1017 UT (blue line). Negative velocities are away from the radar.

The SuperDARN radar data allow us to set the western edge of the reconnection line. Figure 4b shows a radial velocity map from the HAN radar at 0958 UT during a burst of reconnection and the footprint of the MMS spacecraft from 0957 UT to 1017 UT. Large negative velocities are observed to the east together with positive velocities in the western part of the field of view. The transition can be interpreted as the western edge of the reconnection line. The transition in flows occurs at ~21° longitude. The Tsyganenko 96 (T96) model is used to map the MMS spacecraft footprint to the ionosphere. The solid blue dot represents the starting point (~26° longitude) of the MMS trajectory. All four MMS spacecraft are being shown as a single point because of their close formation.

The MMS footprint does not exactly pass through the reconnection region where a strong negative flow (red) is observed. However, we can define the reconnection line as stretching from the transition in flows to the point on the ground which maps to 0.5 R_E east of the spacecraft. The reconnection line has a finite longitudinal extent about 1.5 R_E (~7.6°) if the subsolar magnetopause is located at 11 R_E. This allows both hydrogen and helium ions to escape into the magnetosheath along reconnected field lines.

The results of the mapping are very sensitive to the magnetic field models and IMF/solar wind conditions. In particular, there is a large degree of uncertainty in mapping the magnetic footprints of the MMS spacecraft associated with input parameters used for solar wind conditions. The IMF B_y measured by ARTEMIS P2 was ~1 nT from 0940 UT to 1000 UT and 15 nT B_y was observed by MMS in the magnetosheath. We adjusted IMF B_y input (6.5 nT) to the T96 model for MMS to be located close to the eastern edge of the field of view of the SuperDARN radar. A suitable range of IMF B_y for the field line mapping is between 6 nT and 6.7 nT.

4. Summary and Conclusions

A burst of energetic (~50–1000 keV) proton, helium, and oxygen ions was observed by the EPD investigation on NASA's MMS mission in the magnetosheath just outside subsolar magnetopause between 0957 UT and 1005 UT on 8 December 2015. As the magnetopause receded inward, this burst of energetic ions exhibited an inverse energy dispersion, with the lowest energy ions appearing first. Angular distributions (polar angle versus azimuthal angle) of the energetic ions demonstrated that the energetic ions originated from the magnetosphere.

The rapid inward magnetopause motion was caused by a foreshock solar wind dynamic pressure pulse inferred to have occurred during an interval of nearly radial IMF. The observed inverse energy dispersion signatures can be explained as the effect of a transient solar wind dynamic pressure pulse that energized particles in the outer magnetosphere via betatron acceleration just before they escape. Ground signatures from low-latitude magnetometers confirm the arrival of a solar wind dynamic pressure impulse. From the

estimated magnetopause displacement, we expect a doubling in outer magnetospheric magnetic field strength and energetic particle energies, as observed.

Since reconnection flows attended the magnetopause crossing, we attribute the inversely energy-dispersed betatron-accelerated energetic ions observed in the magnetosheath to escape along reconnected magnetic field lines. As indicated by SuperDARN radar observations of strong antisunward flow, the solar wind dynamic pressure impulse triggered a burst of reconnection. Using combined ground radar and MMS/EIS observations, we estimated a longitudinal extent (~1.5 R_E) for this burst of reconnection. Based on the fact that all three ion species were observed, the distance of the MMS spacecraft from the eastern edge of the reconnection line should not be greater than ~0.5 R_E. The western edge of the reconnection line can be determined from the transition in convection flows observed by the radar.

Acknowledgments
We thank the FGM, FPI, and EPD instrument teams of MMS mission and ARTEMIS mission for the successful spacecraft operation and for providing plasma and magnetic field data. This research was supported by an appointment to the NASA Postdoctoral Program appointment at the NASA/GSFC, administered by Universities Space Research Association through a contract with NASA. Some of the work conducted at NASA/GSFC was supported by the MMS project. J.M.R. acknowledges the support of NSF under AGS-1341918. M.L. is supported by NERC grant NE/K011766/1. The SuperDARN radars are funded by the national scientific agencies of Australia, Canada, China, France, Japan, South Africa, United Kingdom, and the United States. We thank the team of Katie Herlingshaw, Suzie Imber, Hammed Lawal, Tim Yeoman, Jasmine Sandhu, Rosie Johnson, and Timothy David at the University of Leicester who collected the Hankasalmi radar data used in this paper which supported the CAPER rocket campaign. We thank the national institutes that support them and INTERMAGNET for promoting high standards of magnetic observatory practice. We also thank E. Yizengaw, E. Zesta, M.B. Moldwin, and the rest of the AMBER team for the data. AMBER is operated by Boston College and funded by NASA and AFOSR. The *Kp* and *Dst* indices were provided by the website (http://wdc.kugi.kyoto-u.ac.jp/).

References

Burch, J. L., T. E. Moore, R. B. Torbert, and B. L. Giles (2015), Magnetospheric multiscale overview and science objectives, *Space Sci. Rev.*, *199*(1), 5–21, doi:10.1007/s11214-015-0164-9.

Crooker, N. U., C. T. Russell, T. E. Eastman, L. A. Frank, and E. J. Smith (1981), Energetic magnetosheath ions and the interplanetary magnetic field orientation, *J. Geophys. Res.*, *86*, 4455–4460, doi:10.1029/JA086iA06p04455.

Fairfield, D. H., W. Baumjohann, G. Paschmann, H. Luehr, and D. G. Sibeck (1990), Upstream pressure variations associated with the bow shock and their effects on the magnetosphere, *J. Geophys. Res.*, *95*, 3773–3786.

Freeman, T. J., and G. K. Parks (2000), Fermi acceleration of suprathermal solar wind oxygen ions, *J. Geophys. Res.*, *105*, 15,715–15,727.

Fuselier, S. A., D. M. Klumper, and E. G. Shelley (1991), Ion reflection and transmission during reconnection at the Earth's subsolar magnetpause, *Geophys. Res. Lett.*, *16*, 139–142.

Kazama, Y., and T. Mukai (2003), Multiple energy-dispersed ion signatures in the near-Earth magnetotail: Geotail observation, *Geophys. Res. Lett.*, *30*, 1384, doi:10.1029/2002GL016637.

Kudela, K., D. G. Sibeck, M. Slivka, S. Fischer, V. N. Lutsenko, and D. Venkatesan (1992), Energetic electrons and ions in the magnetosheath at low and medium latitudes—Prognoz 10 data, *J. Geophys. Res.*, *97*, 14,849–14,857, doi:10.1029/92JA01134.

Lee, M. A. (1982), Coupled hydromagnetic wave excitation and ion acceleration upstream of the Earth's bow shock, *J. Geophys. Res.*, *87*, 5063–5080.

Lockwood, M., W. F. Denig, A. D. Farmer, V. N. Davda, S. W. H. Cowley, and H. Luehr (1993), Ionospheric signatures of pulsed reconnection at the Earth's magnetopause, *Nature*, *361*, 424–428, doi:10.1038/361424a0.

Mauk, B. H. (1986), Quantitative modeling of the convection surge mechanism of ion acceleration, *J. Geophys. Res.*, *91*, 13,423–13,431.

Mauk, B. H., et al. (2014), The energetic particle detector (EPD) investigation and the energetic ion spectrometer (EIS) for the magnetospheric multiscale (MMS) mission, *Space Sci. Rev.*, *199*(1–4), 471–514, doi:10.1007/s11214-014-0055-5.

Pinnock, M., A. S. Rodger, J. R. Dudeney, K. B. Baker, P. T. Neweli, R. A. Greenwald, and M. E. Greenspan (1993), Observations of an enhanced convection channel in the cusp ionosphere, *J. Geophys. Res.*, *98*, 3767–3776, doi:10.1029/92JA01382.

Quinn, J. M., and C. E. McIlwain (1979), Bouncing ion clusters in the Earth's magnetosphere, *J. Geophys. Res.*, *84*, 7365–7370, doi:10.1029/JA084iA12p07365.

Quinn, J. M., and D. J. Southwood (1982), Observations of parallel ion energization in the equatorial region, *J. Geophys. Res.*, *87*, 10,536–10,540, doi:10.1029/JA087iA12p10536.

Reeves, G. D., T. A. Fritz, T. E. Cayton, and R. D. Belian (1990), Multi-satellite measurements of substorm injection region, *Geophys. Res. Lett.*, *17*, 2015–2018.

Roederer, J. G. (1970), *Dynamics of Geomagnetically Trapped Radiation*, Springer-Verlag, New York.

Russell, C. T., et al. (2014), The magnetospheric multiscale magnetometers, *Space Sci. Rev.*, *199*, 189–256, doi:10.1007/s11214-014-0057-3.

Sauvaud, J.-A., D. Popescu, D. C. Delcourt, G. K. Parks, M. Brittnacher, V. Sergeev, R. A. Kovrazhkin, T. Mukai, and S. Kokubun (1999), Sporadic plasma sheet ion injections into the high-altitude auroral bulge: Satellite observations, *J. Geophys. Res.*, *104*, 28,565–28,586, doi:10.1029/1999JA900293.

Scholer, M., F. M. Ipavich, G. Gloeckler, D. Hovestadt, and B. Klecker (1981), Leakage of the magnetospheric ions into the magnetosheath along reconnected field lines at the dayside magnetopause, *J. Geophys. Res.*, *86*, 1299–1304.

Sibeck, D. G. (1993), Transient magnetic field signatures at high latitudes, *J. Geophys. Res.*, *98*, 243–256, doi:10.1029/92JA01661.

Sibeck, D. G., and R. W. McEntire (1988), Multiple satellite observations of leakage of particles to the magnetosphere, *Adv. Space Res.*, *8*, 201–216.

Sibeck, D. G., R. W. McEntire, A. T. Y. Lui, R. E. Lopez, and S. M. Krimigis (1987a), Magnetic field drift shell splitting: Cause of unusual dayside particle pitch angle distributions during storms and substorms, *J. Geophys. Res.*, *92*, 13,485–13,497.

Sibeck, D. G., R. W. McEntire, A. T. Y. Lui, R. E. Lopez, S. M. Krimigis, R. B. Decker, L. J. Zanetti, and T. A. Potemra (1987b), Energetic magnetospheric ions at the dayside magnetopause: Leakage or merging?, *J. Geophys. Res.*, *92*, 12,097–12,114.

Sibeck, D. G., R. W. M. S. M. Krimigis, and D. N. Baker (1988), The magnetosphere as a sufficient source for upstream ions on November 1, 1984, *J. Geophys. Res.*, *93*, 14,328–14,342.

Sibeck, D. G., W. Baumjohann, R. C. Elphic, D. H. Fairfield, and J. F. Fennell (1989), The magnetospheric response to 8-minute period strong-amplitude upstream pressure variations, *J. Geophys. Res.*, *94*, 2505–2519, doi:10.1029/JA094iA03p02505.

Torbert, R. B., et al. (2014), The FIELDS instrument suite on MMS: Scientific objectives, measurements, and data products, *Space Sci. Rev.*, *199*(1–4), 105–135, doi:10.1007/s11214-014-0109-8.

Wilken, B., C. K. Goertz, D. N. Baker, P. R. Higbie, and T. A. Fritz (1982), The SSC on July 29, 1997 and its propagation within the magnetosphere, *J. Geophys. Res.*, *87*, 5901–5910.

Wilken, B., D. N. Baker, P. R. Higbie, T. A. Fritz, W. P. Olson, and K. A. Pfitzer (1986), Magnetospheric configuration and energetic particle effects associated with a SSC: A case study of the CDAW Event on March 22, 1979, *J. Geophys. Res.*, *91*, 1459–1473.

Zong, Q.-G., and B. Wilken (1998), Layered structure of energetic oxygen ions in the magnetosheath, *Geophys. Res. Lett.*, *25*, 4121–4124.
Zong, Q.-G., B. Wilken, J. Woch, G. Reeves, T. Doke, and T. Yamamoto (1999), Energetic particle bursts in the near-Earth magnetosheath during a storm, *Phys. Chem. Earth*, *24*, 293–298.
Zong, Q.-G., B. Wilken, S.-Y. Fu, T. A. Fritz, Z.-Y. Pu, N. Hasebe, and D. J. Williams (2001), Ring current oxygen ions in the magnetosheath caused by magnetic storm, *J. Geophys. Res.*, *106*, 25,541–25,556.